

A Combined Analytical and Numerical Approach for the Evaluation of Radial Loads on the Lining of Vertical Shafts

*Original*

A Combined Analytical and Numerical Approach for the Evaluation of Radial Loads on the Lining of Vertical Shafts / Oreste, Pierpaolo; Spagnoli, Giovanni; LO BIANCO, Luigi. - In: GEOTECHNICAL AND GEOLOGICAL ENGINEERING. - ISSN 0960-3182. - STAMPA. - 34:4(2016), pp. 1057-1065. [10.1007/s10706-016-0026-6]

*Availability:*

This version is available at: 11583/2648574 since: 2016-09-13T11:18:46Z

*Publisher:*

Springer International Publishing

*Published*

DOI:10.1007/s10706-016-0026-6

*Terms of use:*

This article is made available under terms and conditions as specified in the corresponding bibliographic description in the repository

*Publisher copyright*

(Article begins on next page)

1 **A combined analytical and numerical approach for the evaluation of radial loads on**  
2 **the lining of vertical shafts**

3 Pierpaolo Oreste<sup>1</sup>, Giovanni Spagnoli<sup>2,3</sup>, Luigi Lo Bianco<sup>1</sup>

4 <sup>1</sup> Department of Environmental, Land and Infrastructural Engineering, Politecnico di Torino,  
5 Corso Duca Degli Abruzzi 24, 10129 Torino, Italy

6 <sup>2</sup> Department of Maritime Technologies, BAUER Maschinen GmbH, Schrobenhausen, Ger-  
7 many

8 \* corresponding author, Tel: +49 8252 972313, Email: [giovanni.spagnoli@bauer.de](mailto:giovanni.spagnoli@bauer.de)

9 <sup>3</sup> Adjunct lecturer, School of Civil, Structural and Environmental Engineering, University Col-  
10 lege Dublin, Dublin, Ireland

11 **ABSTRACT**

12 The evaluation of the load acting on a shaft support is of fundamental importance for the cor-  
13 rect dimensioning of the structure. The load acting on the support can appear somewhat  
14 complex. One approach may be to use the convergence-confinement method (CCM) normal-  
15 ly used in the tunneling design. This process involves intersecting the convergence-  
16 confinement (CC) curve with the support reaction line. However, in order to be able to adopt  
17 this technique, it is necessary to know the radial displacement of the shaft wall at the point in  
18 which the support is to be installed. Using the equations of Vlachopoulos and Diederichs  
19 (2009) the reaction line of the support can be calculated. Numerical models developed with  
20 Flac 2D v.6.0 considering the Mohr-Coulomb criterion and an ideal elastic-plastic behavior  
21 simulating stepwise excavation and support installation were developed. The relation be-  
22 tween applied internal stress and radial displacement of the wall shaft, obtained by the nu-  
23 merical simulation was compared with the CC curve obtained by the CCM and it showed a  
24 good match between the two methods. However, an iterative procedure has also been used  
25 to insert the reaction line in the CC graph. The result shows lower initial displacements (and  
26 therefore greater radial stress) when compared with the values obtained by numerical calcu-  
27 lation with the axisymmetric model. It is therefore recommended the combined use of the

28 CCM (analytical method) and the axisymmetric numerical model (step by step simulation) to  
29 obtain the values of the final load on the lining and the final plastic radius, necessary for the  
30 correct design of supporting structures on the shaft wall.

31 **Key words:** shaft, lining, convergence-confinement method, FLAC, weak rocks, numerical  
32 modelling, axisymmetric model, wall radial displacement profile.

33

## 34 **Introduction**

35 Underground mining methods invariably rely on tunneling networks to gain access to the  
36 zones of valuable minerals (Carter et al. 2011). Underground mines can be reached via  
37 ramps, inclined or vertical shafts or adits (Bullock 2011). To achieve great depths, vertical  
38 shafts are created. The method used to date for the construction of shaft is the shaft sinking  
39 (drill and blast), however over the past recent years, the mechanical excavation has become  
40 remarkably common, especially in underground mining (Rostami 2011). Depths up to 1,000m  
41 can be achieved through the conventional method whereas deep shafts up to 2,000m can be  
42 reached through mechanical method. The mechanical method has besides several ad-  
43 vantages over the conventional method such as (Bullock 2011):

- 44 • Improved personal safety;
- 45 • Minimal ground disturbance;
- 46 • Less material to move;
- 47 • Uniform muck size;
- 48 • Continuous operations;
- 49 • Conducive to automation of system;
- 50 • Higher production rates.

51 Research into shaft construction is now becoming of increasing importance. Because ore  
52 bodies are becoming depleted, shafts are being constructed ever deeper and in ever more  
53 challenging geologies such as weak rocks. Studies carried out on these rocks show a rock  
54 intumescent, which can easily be damaged (Guo et al. 2012). Stress testing and analysis of  
55 structural geology must be taken into account for a correct mechanical characterization of the  
56 rock. Design methods for shaft lining are therefore very important. Jia et al. (2013) described  
57 the case of the Boulby Potash Mine where shaft linings installed in Marl suffered considera-  
58 ble radial pressure from the Marl stratum together with vertical compression from the upper  
59 part of the shafts resulting from subsidence of the host surrounding rock.

60 The main objectives of the linings are to maintain stability and preserve the ability of stress-  
61 carrying rocks near the boundaries of underground excavations. Different types of reinforce-  
62 ment may be used for this purpose: shotcrete, mesh, steel, concrete sets, and reinforced  
63 concrete linings. In literature many design methods for shafts exist. The calculation of the  
64 lining thickness for circular wells is based on the assumption that the pressure on the contact  
65 rock-lining is known (Öztürk and Ünal 2001). In general, according to Wong and Kaiser  
66 (1988), the design of a shaft consists of:

- 67 1. The design of the shaft lining to prevent instability of shaft wall and;
- 68 2. Estimation of the soil movement associated with shaft construction.

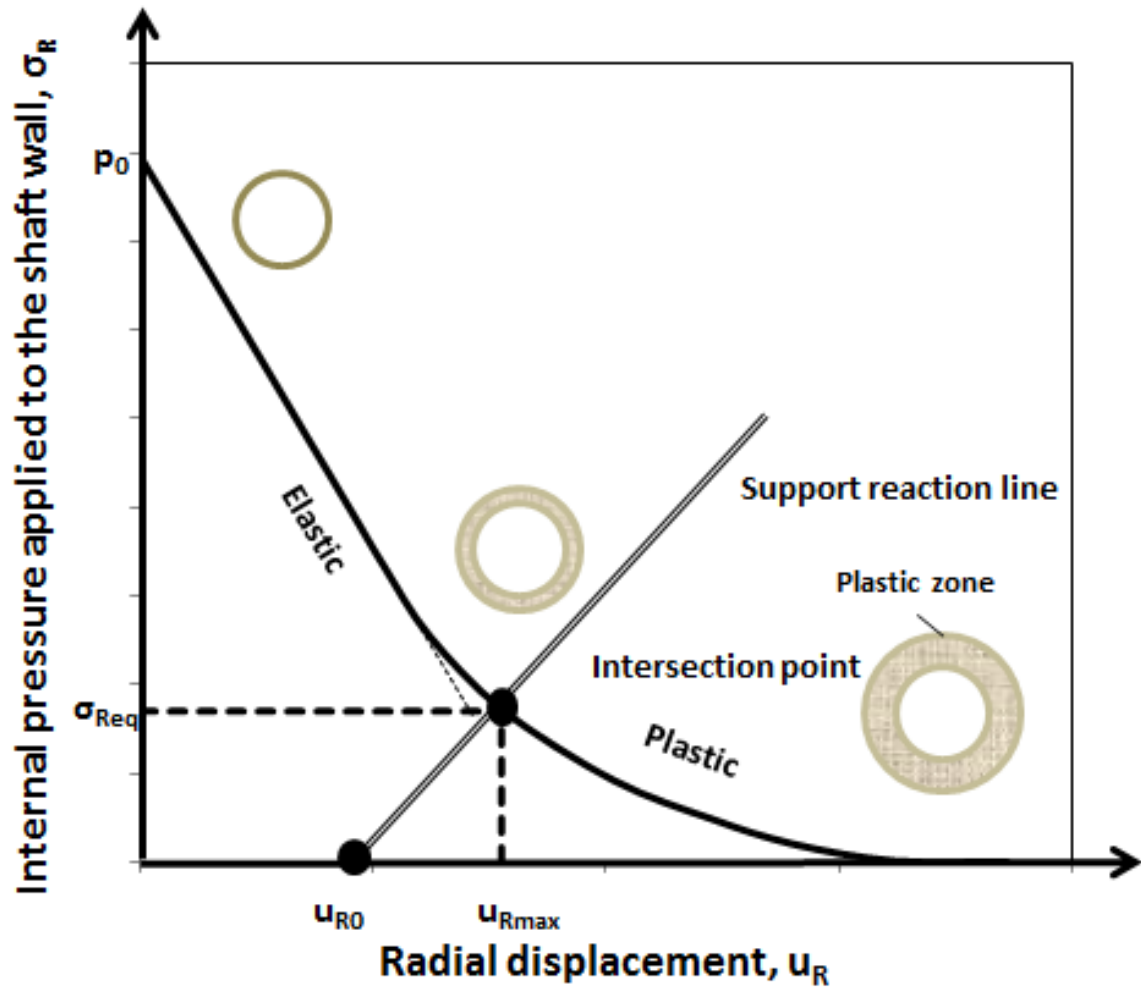
69 Although these two tasks are interrelated, they are usually handled separately. According to  
70 Wong and Kaiser (1988) many design approaches are based on soil plasticity considering  
71 the stress redistribution around a circular shaft opening (see Terzaghi 1943). Berezantzev  
72 (1958) used the Mohr-Coulomb failure criterion as a condition of plastic equilibrium and also  
73 made the assumption of equal principal stresses to render the problem statically determinate.  
74 The yield zone considered by Berezantzev (1958) is bounded by Rankine slip lines. Alterna-  
75 tively Coulomb-type analysis with a conical sliding surface are also used (e.g. Prater 1977).  
76 Both shaft design model consider gravity or the influence of the vertical principal stress. An-  
77 other method is the one treating a shaft as a two dimensional *hole-in-a-plate* model in order  
78 to calculate the extent of yielding, the equilibrium support pressure, and the related defor-  
79 mations for circular openings in a uniform stress field and in perfectly plastic or strain-  
80 weakening ground (e.g. Abel et al. 1979; Brown et al. 1986). The actually expected and ob-  
81 served pressures depend, however, on such factors as ground deformation, in situ stress,  
82 and ground strength-deformation properties. However, as stated by Wong and Kaiser (1988)  
83 the methods described above describe the actual shaft behavior. These methods do not indi-  
84 cate when gravity effects are relevant or when the limits of applicability of the "hole-in-a-  
85 plate" approach have been reached. McCreath (1980) found that the convergence-

86 confinement method (CCM) could be applied to explain the shaft performance of deep shaft  
87 in yielding rocks.

88 In this research the main analytical methods used in the calculation of the loads acting on the  
89 shaft lining and two-dimensional numerical models of the cross section and longitudinal sec-  
90 tion (axisymmetric modelling) are presented. The comparison of the calculation results for a  
91 specific case will permit to obtain useful indications on the optimal calculation technique in  
92 order to correctly assess the radial load on the lining and to design it.

### 93 **The convergence-confinement method and the equation of Vlachopoulos and** 94 **Diederichs for the evaluation of the radial displacement profile**

95 The CCM method is one of the most commonly used analytical methods in the field of tunnel-  
96 ing (Fig. 1). It permits to analyze the stresses and strains that develop around a deep circular  
97 cavity. The extent of the yield (or plastic) zone can also be estimated by this method under  
98 well-defined conditions (e.g. Fenner 1939; Pacher 1964; Rechsteiner and Lombardi 1974).  
99 This method requires the intersection of the convergence-confinement (CC) curve with the  
100 support reaction line. The value of the radial stress acting at the extrados of the support  
101 structure is an important result that can be obtained (Oreste 2005a; 2005b). The CCM was  
102 adopted and proposed by Wong and Kaiser (1988) as a rational approach to predict shaft  
103 behavior. In this manner in situ stress, rock strength, and deformation properties as well as  
104 many construction details can be included in the analysis.



105

106 Fig. 1 Convergence-confinement curve of an underground opening and the reaction line of  
 107 the support (modified after Vlachopoulos and Diederichs 2009). Key:  $p_0$  is the lithostatic  
 108 stress,  $u_{R0}$  is the radial wall displacement in the point along the cavity axis where the lining is  
 109 constructed,  $u_{Rmax}$  is the final radial wall displacement of the cavity,  $\sigma_{Req}$  is the final radial load  
 110 on the lining.

111 The assumptions used in the development of the CCM are:

- 112 • Circular and deep shaft;
- 113 • Homogeneous and isotropic rock around the shaft;
- 114 • Isotropic lithostatic stress around the shaft, with the horizontal lithostatic stresses  
 115 equal in the two main directions in the case of a vertical shaft (e.g. Panet 1995;  
 116 Oreste 2009a).

117 In order to proceed with the correct evaluation of the load acting on the support with the CC  
 118 curve, it is necessary to know the radial displacements of the shaft walls at the moment in  
 119 which the support structure is installed ( $u_{R0}$ ). The formulation presented by Vlachopoulos and  
 120 Diederichs (2009), which allows an estimation of the radial displacements in function of the  
 121 final radial displacement of the shaft, at a long distance from the excavation face, appears to  
 122 be particularly interesting. This equation allows estimating the radial movement  $u_{R0}$  of the  
 123 shaft wall where the support structure of the shaft is installed (generally near to the excava-  
 124 tion bottom). For Vlachopoulos and Diederichs (2009)  $u_R$  is described by the following equa-  
 125 tion in function of the distance  $x$  from the shaft bottom:

$$126 \frac{u_R}{u_{Rmax}} = 1 - \left(1 - \frac{1}{3} \cdot e^{-0.15 \cdot \frac{R_{pl}}{R}}\right) \cdot e^{\left[\frac{-3 \cdot x}{2 \cdot R_{pl}}\right]} \quad (1)$$

127  
 128 Where:  $u_{Rmax}$  is the maximum radial displacement of the shaft (for very elevated  $x$ );  
 129  $R_{pl}$  is the final plastic radius of the shaft (for very elevated  $x$ );

### 130 **The iterative procedure to design the linings using the convergence confine-** 131 **ment method**

132 In order to insert the reaction line of the support in the CCM, the formulation of Vlachopoulos  
 133 and Diederichs (2009) can be used; this formulation permits to estimate the wall displace-  
 134 ment,  $u_{R0}$ , of the shaft at the point where the supports are installed. Because the radial dis-  
 135 placement and the plastic radius at a great distance from the excavation bottom are influ-  
 136 enced by  $u_{R0}$  (which is unknown) an iterative procedure can be adopted (Oreste 2009b) This  
 137 procedure involves the following steps:

- 138 1. Inserting the reaction line in the graph of the curve obtained by the CCM (Fig. 1), initially  
 139 considering  $u_{R0} = 0$ ; the support reaction line has a slope given by its stiffness  $k_{sup}$  (Hoek  
 140 and Brown 1980):

$$141 k_{sup} = \frac{E_{sup}}{(1+\nu_{sup})} \cdot \frac{R^2 - (R - t_{sup})^2}{(1 - 2\nu_{sup}) \cdot R^2 + (R - t_{sup})^2} \cdot \frac{1}{R} \quad (2)$$



142 where:  $R$  is the shaft radius;  
143  $t_{sup}$  is the lining thickness;  
144  $E_{sup}$  e  $\nu_{sup}$  are the elastic modulus and Poisson ratio of the lining material respec-  
145 tively.

- 146 2. Determination of the intersection point of the convergence-confinement curve with the  
147 reaction line of the lining, obtaining the first value of the final shaft wall displacement  
148 ( $u_{Rmax}$ ) and determining the final pressure applied to the lining ( $\sigma_{Req}$ ), at a great distance  
149 from the temporary bottom.
- 150 3. Calculation of the plastic radius,  $R_{pl}$ , which develops at a great distance from the tempo-  
151 rary excavation bottom, starting from  $\sigma_R$  as determined above.
- 152 4. Estimation of  $u_{R0}$  through Equation 1 knowing  $u_{Rmax}$  and  $R_{pl}$  obtained from steps 2 and 3.  
153 The distance from the shaft bottom,  $x$ , is replaced by the actual distance from the tempo-  
154 rary shaft bottom, where the support is installed.
- 155 5. The new value of  $u_{R0}$  is used to re-calculate the position of the reaction line, by repeating  
156 steps 2 to 4.

157 The iterative procedure rapidly converges and can be stopped when the difference between  
158 two consecutive values of  $u_{R0}$  or  $\sigma_{Req}$  is below a certain predetermined tolerance. After this  
159 procedure it is possible to obtain in the convergence-confinement curve graph, the position of  
160 the reaction line according to the equation of Vlachopoulos and Diederichs (2009). The inter-  
161 section between the two curves allows calculating both the final displacement of the shaft  
162 wall and the final radial load acting on the lining. This in turn, quickly permits the verification  
163 about the ability of the lining to sustain the rock pressure, without using any numerical model.  
164 This approach could be useful in the determination of the shaft lining type and consistency,  
165 until reaching a final configuration that guarantees not only shaft walls stability but also the  
166 optimization of the available economic resources.

## 167 **Numerical simulations of the shaft installation**

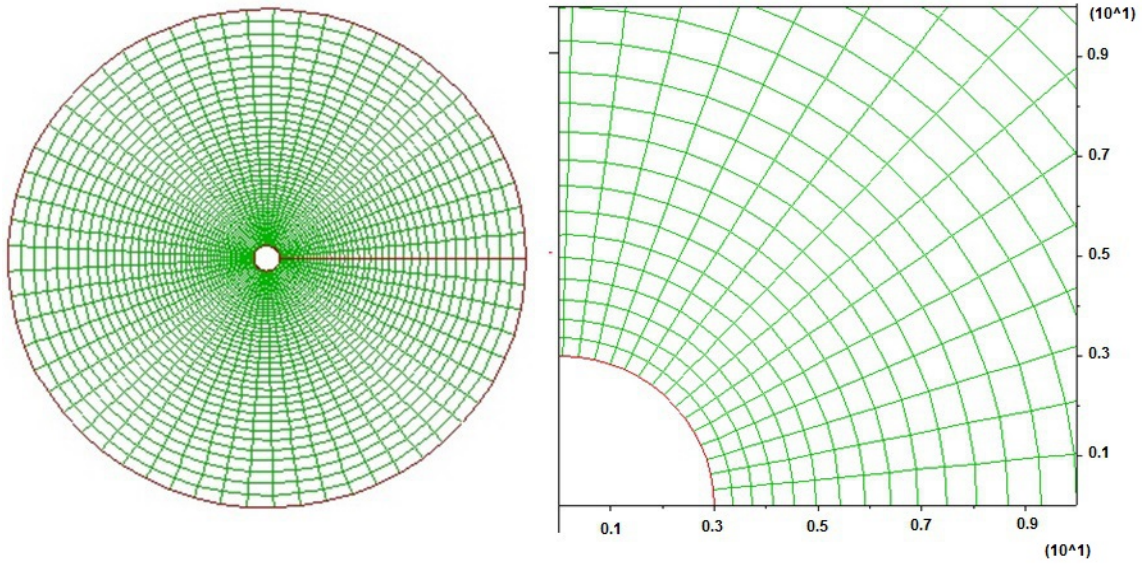
168 The shaft installation can be studied in great detail by the two-dimensional numerical model-  
169 ing when the lithostatic state has equivalent horizontal stress in the two main directions and  
170 when the section of the shaft is assumed to be circular. In fact, in this case, it is possible to  
171 study the cross section with a plane model (plane strain state condition) and the longitudinal  
172 section (vertical section) with an axisymmetric model. The combined use of these two numer-  
173 ical models permits to have all the necessary information on the stress and strain developing  
174 in the rock mass around the shaft and in the lining.

175 This paragraph analyzes, with the combined use of the two-dimensional modeling, the stress  
176 and strain at the shaft contour considering a circular section with 3m radius. Assuming the  
177 Mohr-Coulomb strength criterion and an ideal elastic-plastic behavior, the following mechani-  
178 cal properties of the rock mass were considered in the studied case:

- 179 • cohesion (c): 0.9MPa;
- 180 • friction angle ( $\varphi$ ): 31°;
- 181 • elastic modulus (E): 8000MPa;
- 182 • Poisson ratio ( $\nu$ ): 0.3.

183 Lithostatic stress was assumed to be equal to 15MPa, in both vertical and in two main hori-  
184 zontal directions (isotropic stress conditions). This stress state refers to conditions that may  
185 be encountered at a depth of about 650-700m.

186 The numerical models were developed with the numerical code FLAC 2D v.6.0 (Flac 2008),  
187 which uses a finite differences numerical solution. The two-dimensional numerical model of  
188 the plane section considers 2745 quadrilateral elements and represents a rock portion at the  
189 shaft contour up to the distance of 60m (Fig. 2).

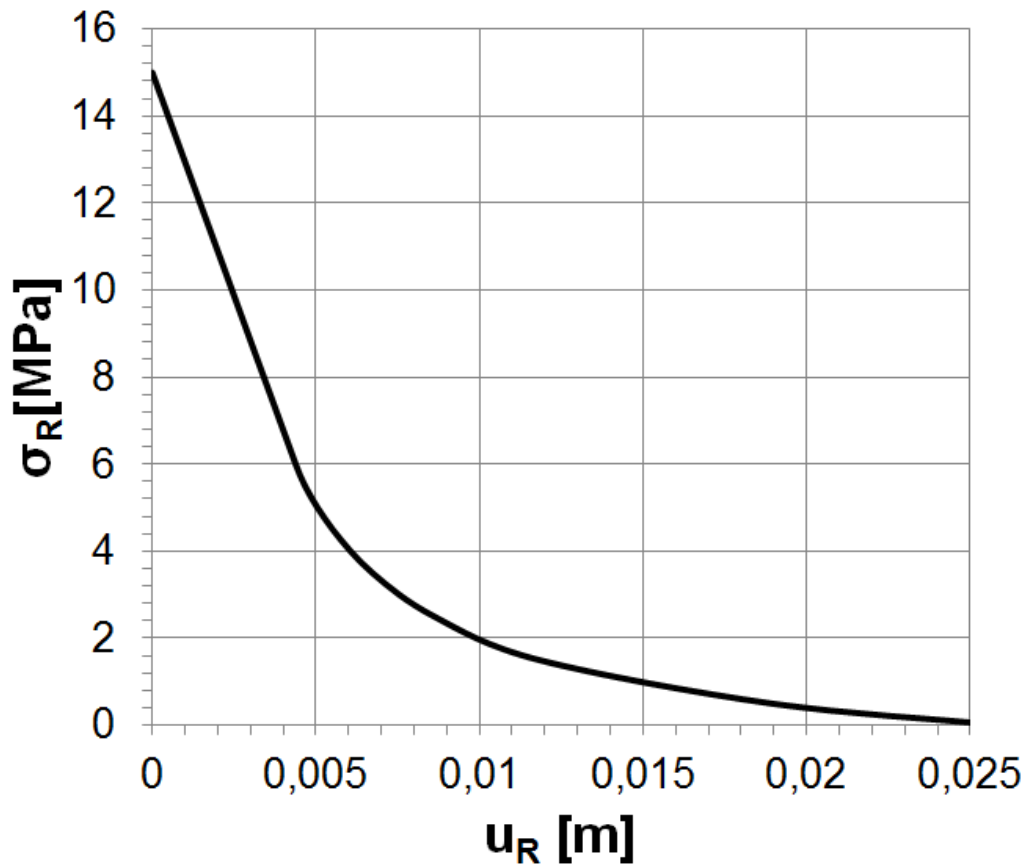


190

191 Fig. 2. Two-dimensional numerical model of the plane section. Left: the whole model; Right:  
192 a detail of the zone close to the shaft wall.

193

194 The internal pressure at shaft has been reduced from the lithostatic value of 15MPa to 0MPa,  
195 for 0.5MPa intervals (to simulate the excavation process) in order to obtain a detailed rela-  
196 tionship between the radial displacement of the shaft wall and the internal pressure (Fig. 3).

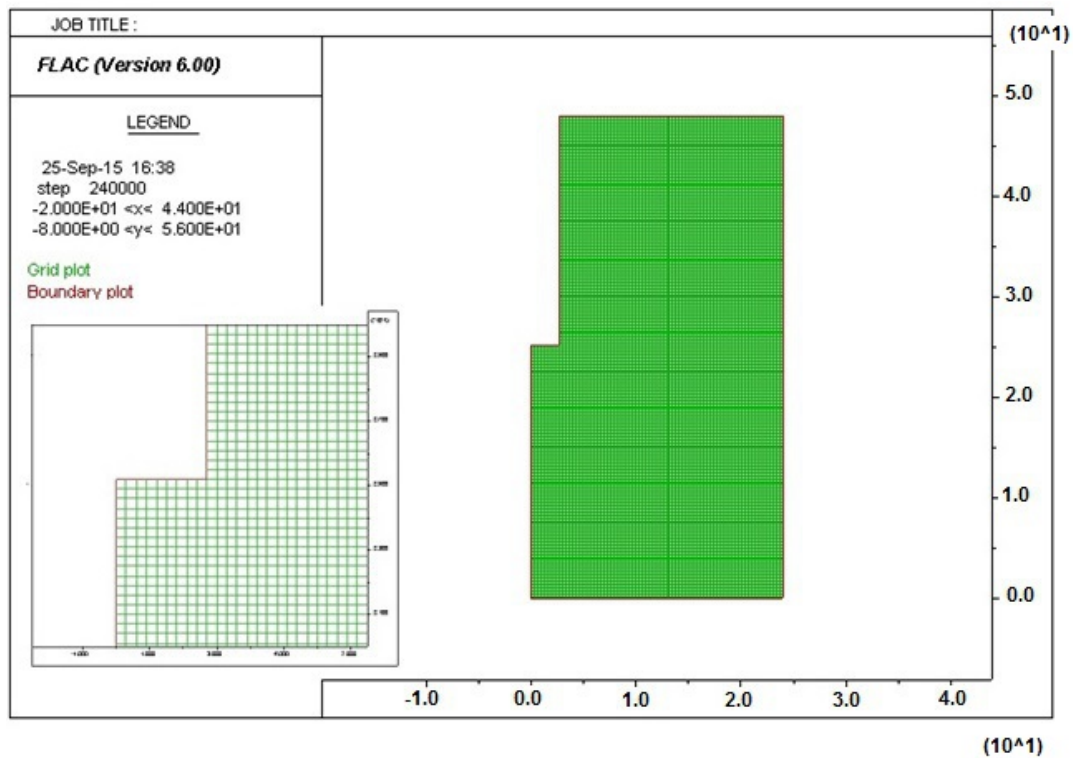


197

198 Fig 3. Relationship between the radial displacement of the shaft wall  $u_R$  and the internal  
 199 pressure for the studied case  $\sigma_R$  obtained by the numerical modeling of the cross-section

200

201 The axisymmetric numerical model simulated a vertical longitudinal section of half shaft, for  
 202 48m depth and 24m width (i.e. 16 times the shaft radius) (Fig. 4). The quadrilateral elements  
 203 used for the analysis (about 12,800 items) have dimension 0.3m side and square in shape.



204

205 Fig 4. Element mesh of the axisymmetric numerical model of the half shaft longitudinal sec-  
 206 tion: the global view and a detail of the zone of the model close to the temporary shaft bot-  
 207 tom.

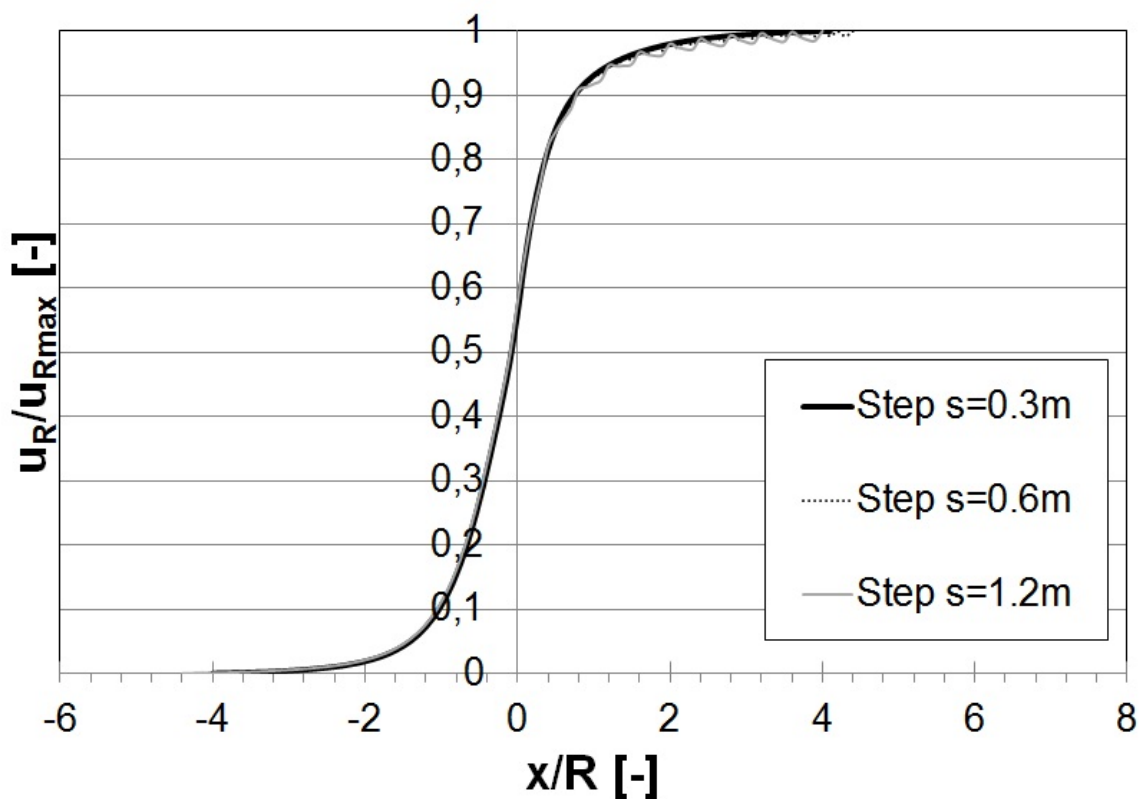
208

209 Through the axisymmetric numerical model, it was possible to simulate both excavation op-  
 210 erations and lining installation, along the entire depth of the model, proceeding from the up-  
 211 per edge until reaching the bottom edge. Different excavation and support step lengths were  
 212 considered: 0.3, 0.6 and 1.2m.

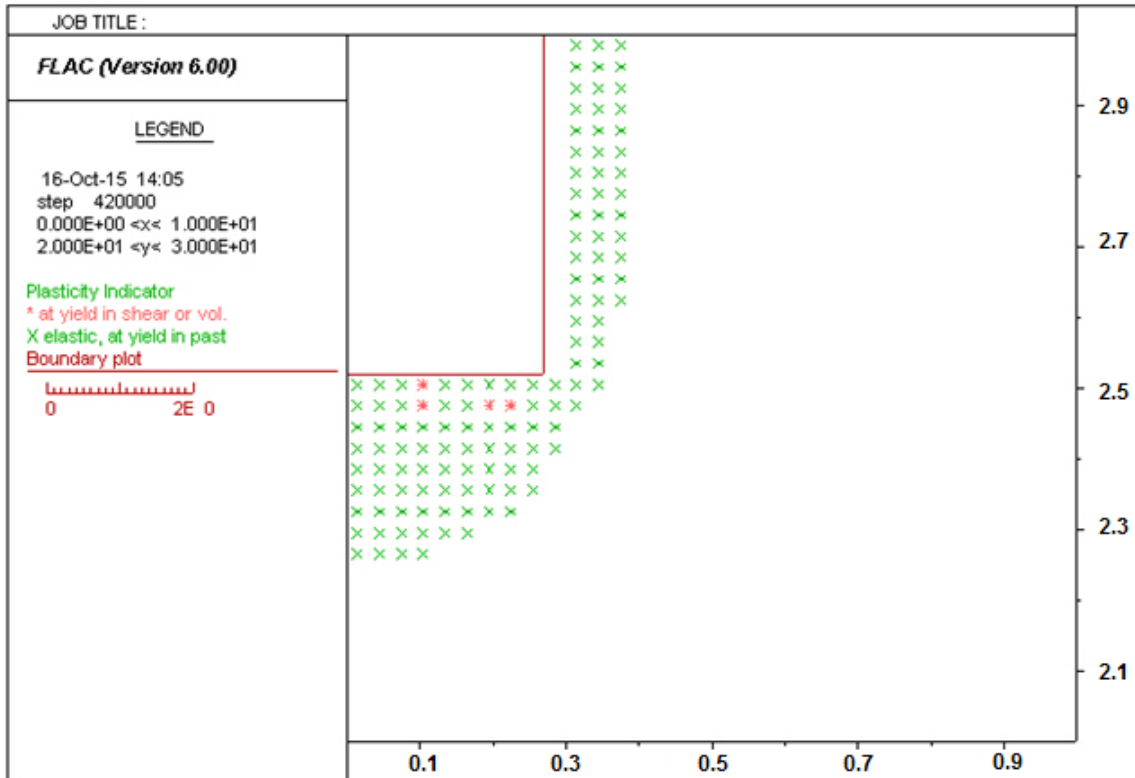
213 The lining was considered immediately active after the completion of the excavation. The  
 214 excavation was simulated through the cancellation of model elements in the shaft zone. The  
 215 lining considered in the calculation consists of concrete (with  $E=25000\text{MPa}$  and  $\nu=0.15$ ) and  
 216 it was simulated by the same elements of the numerical model, reactivated after the cancel-  
 217 lation with the mechanical characteristics of the concrete and with a zero initial stress state.

218 The situation obtained by the calculation with the bottom of the excavation positioned at half  
 219 depth of the model, was analyzed with great detail. It was possible to detect the trend of the  
 220 radial displacement of the wall shaft, obtained by the numerical calculation at different dis-

221 tances from the excavation bottom. This trend seems to be of great interest because it repre-  
222 sents the deformation condition of the shaft in the radial direction, with the presence of lining  
223 in the section already excavated (Fig. 5). From the analysis shown in Fig. 5 it is possible to  
224 observe how the radial displacement from the shaft wall is less influenced by the excavation  
225 steps,  $s$ . In addition to the conditions of deformation, also the plastic zones, observed during  
226 the calculation, were analyzed: more specifically a final plastic radius of 3.9 m was observed  
227 for each analyzed excavation step (Fig. 6).



228  
229 Fig 5 Deformation condition of the shaft in the radial direction, with the presence of lining, in  
230 the section already excavated with different step values,  $s$ . Key:  $u_R$  is the radial displacement  
231 of the shaft wall,  $u_{Rmax}$  is the maximum radial displacement at a great distance from the shaft  
232 bottom,  $R$  is the shaft radius.

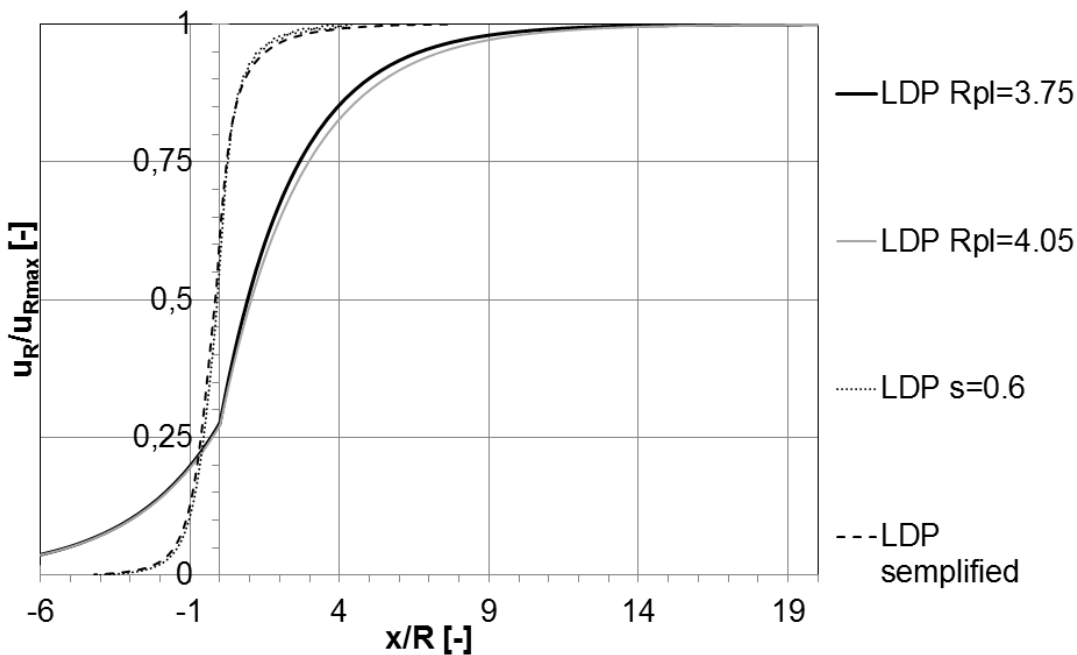


233

234 Fig 6. Plastic zones around the shaft and below the shaft bottom during the axisymmetric  
 235 numerical calculation: a final plastic radius  $R_{pl}$  in the interval between 3.75 m and 4.05 m can  
 236 be estimated by the results.

237 Fig. 7 shows the comparison of the curves shown in Fig. 5 (for  $s = 0.6\text{m}$ ) and the result from  
 238 the simplified excavation simulation, obtained by instantaneously eliminating all the elements  
 239 until reaching the half of the model, with the simultaneous activation of the support along the  
 240 excavated section. The instantaneous shaft excavation for half depth, without simulating the  
 241 excavation and support installation steps, performed in the previous analyses, was therefore  
 242 simulated. In Fig. 7 also the radial displacements of the shaft walls obtained using the equa-  
 243 tion of Vlachopoulos and Diederichs (2009) are shown, considering the displacement  $u_{R_{max}}$   
 244 and two different values of the final plastic radius  $R_{pl}$ , all obtained by the numerical simula-  
 245 tion. The two extreme values of plastic radius (i.e. 3.75 and 4.05m) obtained by the numeri-  
 246 cal modelling, were considered. Analyzing the data of Fig. 7 we can observe:

- 247 1. The simplified shaft excavation and support simulation (“LDP simplified” curve in Fig.  
 248 7) shows a trend for the ratio between radial displacement  $u_R$  and the maximum dis-  
 249 placement  $u_{Rmax}$ , which practically corresponds to the trend obtained with the proce-  
 250 dure considering both excavation and support installation by steps (step by step pro-  
 251 cedure: “LDP s=0.6” curve).
- 252 2. The equation of Vlachoupulos and Diederichs (2009), which is very widespread in  
 253 geomechanical design practice, for  $R_{pl}$  3.75 (black continuous line) and  $R_{pl}$  4.05 (grey  
 254 continuous line) creates radial displacements of shaft walls, which are different from  
 255 the ones obtained by the numerical axisymmetric calculation, even if in the Vla-  
 256 choupulos and Diederichs equation (2009), values of  $u_{Rmax}$  and  $R_{pl}$  obtained by the  
 257 numerical simulation, are used;
- 258 3. In the numerical simulation, the radial wall displacement in correspondence of the  
 259 temporary excavation bottom (where the support is activated) is about 60% of the fi-  
 260 nal displacement; for Vlachoupulos and Diederichs (2009) this value is about 28%,  
 261 i.e. near the half obtained by the numerical simulation.



262

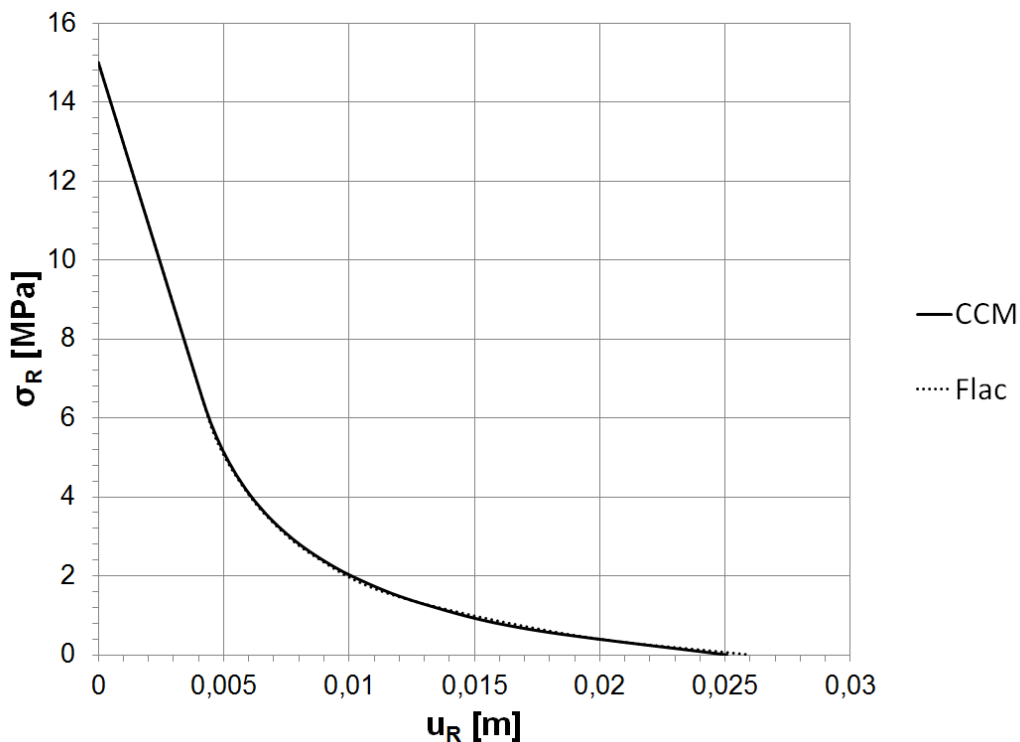
263 Fig. 7. Comparison of the trends of radial displacements of shaft wall with the distance  $x$  from  
 264 the temporary shaft bottom, obtained by the numerical simulation and Vlachoupulos and



265 Diederichs formulation. Key: LDP: longitudinal displacement profile; LDP  $R_{pl}$  3.75: displace-  
266 ment profile obtained by the Vlachopoulos and Diederichs formulation considering a plastic  
267 radius of 3.75 m; LDP  $R_{pl}$  4.05: displacement profile obtained by the Vlachopoulos and  
268 Diederichs formulation considering a plastic radius of 4.05 m; LDP  $s=0.6$ : displacement pro-  
269 file obtained by the step by step axisymmetric numerical calculation for a step length of 0.6m;  
270 LDP simplified: displacement profile obtained by the simplified axisymmetric numerical calcu-  
271 lation.

### 272 Comparison between the analytical iterative procedure and the numerical simulation

273 The relation between the applied internal pressure and the radial displacement of the shaft  
274 wall, obtained by the numerical simulation of the cross-section (see Fig. 3) was compared  
275 with the CC curve of the circular cavity obtained by the CCM (Fig. 8). It is possible to observe  
276 a very good match between the two methods. The CCM represents therefore an interesting  
277 alternative tool to the numerical modeling of the shaft cross-section. The CCM permits to  
278 quickly calculate the CC curve of the circular cavity, in comparison with the numerical model-  
279 ling.

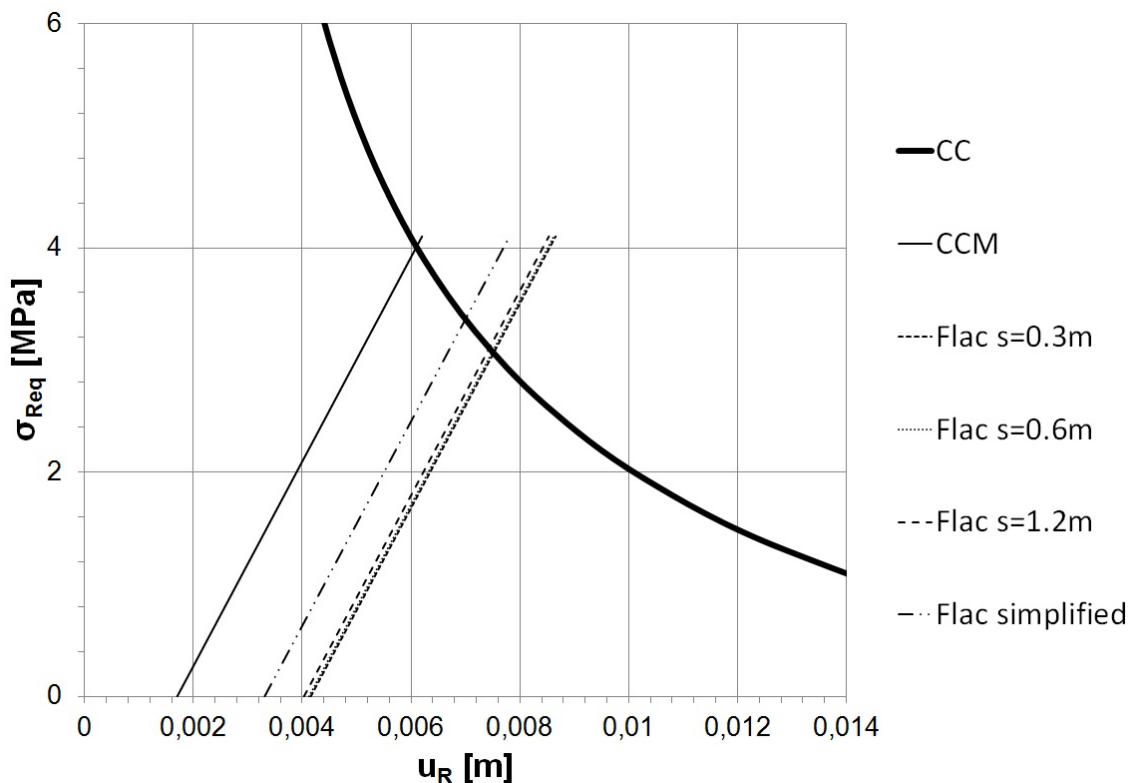


281 Fig. 8. Comparison of the applied internal pressure-radial displacement of the wall shaft  
 282 curve, obtained with FLAC numerical modelling (dotted line) and with the CCM (continuous  
 283 line).

284

285 In the CC graph, the reaction line of the support has been inserted as previously described in  
 286 paragraph 3 (see Fig. 9). The results coming from the iterative procedure give an initial dis-  
 287 placement,  $u_{R0}$ , of 1.7mm and a final radial stress,  $\sigma_{Req}$ , of 4MPa. In Fig. 9 the reaction lines  
 288 of the support obtained from the  $u_{R0}$  values of the axisymmetric models for the following con-  
 289 ditions are also shown:

- 290 • excavation and support installation simulation for steps with length of 0.3, 0.6 and
- 291 1.2m (step by step procedure);
- 292 • Simplified excavation and support installation simulation (“Flac simplified” reaction
- 293 line);



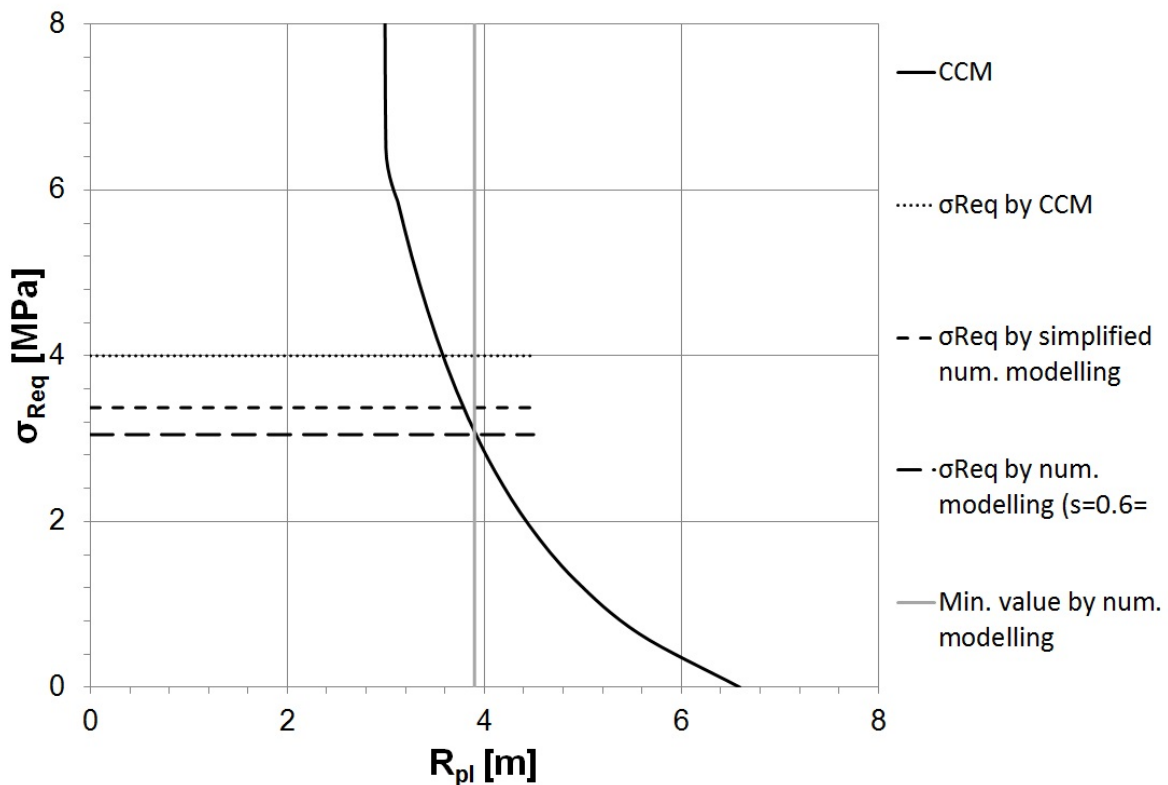
294

295 Fig. 9. Comparison of the support reaction lines obtained with different calculation proce-  
 296 dures. Key: CC: convergence-confinement curve obtained by CCM; CCM: support reaction  
 297 line located on the basis of the iterative procedure of section 3; “Flac s=0.3 m”: support reac-

298 tion line located on the basis of step by step procedure using the axisymmetric numerical  
299 model and a step length of 0.3 m; “Flac s=0.6 m”: step length of 0.6 m; “Flac s=1.2 m”: step  
300 length of 1.2 m; “Flac simplified”: support reaction line located on the basis of the simplified  
301 procedure using the axisymmetric numerical model.

302

303 Comparing the data it is possible to observe how the iterative procedure previously described  
304 in paragraph 3 gives a  $u_{R0}$  value less than 54% and a  $\sigma_{Req}$  value higher than 30% with re-  
305 spect to the three analyzed cases with the axisymmetric numerical model and by considering  
306 the excavation step by step ( $u_{R0} \cong 4.1\text{mm}$ ;  $\sigma_{Req} \cong 3.1\text{MPa}$ ). The different excavation step  
307 values do not appreciably influence  $u_{R0}$  neither does the final stress on the lining,  $\sigma_R$ . The  
308 simplified axisymmetric numerical simulation give intermediate values of  $u_{R0}$  and  $\sigma_R$  with re-  
309 spect to those described above. The value of  $u_{R0}$  is in fact less than 20% and  $\sigma_R$  is higher  
310 than 10% if compared with the step by step simulations. Regarding the final plastic radius,  
311 considered at a long distance from the temporary excavation bottom, we can observe how  
312 the value obtained from the analytical iterative procedure is about 8% less than the one ob-  
313 tained by the axisymmetric numerical simulations (Fig. 10). The value of the plastic radius  
314 calculated by the step by step axisymmetric numerical simulation agrees with the one ob-  
315 tained by the relation  $R_{pl}-\sigma_{Req}$  calculated by means of the CCM. In this case, too, the final  
316 plastic radius is 2% smaller than the one obtained by the step by step axisymmetric numeri-  
317 cal simulation.



318

319 Fig. 10. Calculation of the final plastic radius  $R_{pl}$  obtained with different calculation proce-  
 320 dures. Key: "CCM": plastic radius vs internal pressure curve obtained by CCM; " $\sigma_{Req}$  by-  
 321 CCM": plastic radius obtained by the internal pressure derived by the analytical iterative pro-  
 322 cedure; " $\sigma_{Req}$  by simplified num. modelling": plastic radius obtained by the internal pressure  
 323 derived by the simplified axisymmetric numerical model; " $\sigma_{Req}$  by simplified num. modelling  
 324 ( $s=0.6$ )": plastic radius obtained by the internal pressure derived by the step by step axisim-  
 325 metric numerical model; "Min. value by num. modelling": the plastic radius value obtained by  
 326 the axisymmetric numerical analyses.

### 327 Conclusions

328 The design of the shaft lining is a very important stage in the shaft design. From the results  
 329 coming from the research presented in the paper, the CCM seem to be an interesting tool for  
 330 describing the relation between the applied internal stress and the radial displacement of the  
 331 shaft walls. The CCM could be an alternative calculation method to the 2D numerical model  
 332 for the horizontal cross-section of the shaft.

333 The simplified iterative procedure, used for positioning the reaction line of the support on the  
334 characteristic curve graph of the circular cavity, gives, however, final stress values on the  
335 lining higher (about 30%) with respect to the values obtained with the axisymmetric numeri-  
336 cal model step by step, i.e. simulating the progressive shaft excavation and support installa-  
337 tion. For this reason, a step by step axisymmetric numerical model, in order to obtain the  
338 radial displacement of the shaft wall ( $u_{R0}$ ) in the zone where the lining is installed, was devel-  
339 oped. The simplified axisymmetric numerical model, although it correctly estimates the rela-  
340 tion between  $u_{R0}$  and  $u_{max}$ , it over-estimates the value of the final stress on the lining, giving  
341 higher value than the one obtained with the step by step axisymmetric numerical model.  
342 The combined use of the CCM and the step by step axisymmetric numerical model gave very  
343 good estimation of the final stress on the lining and final plastic radius values, both of them  
344 necessary to correctly design the support structure of the shaft, in order to guarantee its sta-  
345 bility.

#### 346 **References**

- 347 Abel JF, Dowise E, Richards P (1979) Concrete shaft lining design. Proc 20th U.S. Symposi-  
348 um on Rock Mechanics, Austin, TX, pp 627-633.
- 349 Berezantzev VG (1958) Earth pressure on the cylindrical retaining walls. Proc Conference on  
350 Earth Pressure Problems, Brussels, Vol. II, pp 21 -24.
- 351 Brown ET, Bray JW, Ladanyi B, Hoek E (1986) Ground response curves for rock tunnels. J  
352 Geotech Eng ASCE 109:12-23, [http://dx.doi.org/10.1061/\(ASCE\)0733-](http://dx.doi.org/10.1061/(ASCE)0733-9410(1983)109:1(15))  
353 [9410\(1983\)109:1\(15\)](http://dx.doi.org/10.1061/(ASCE)0733-9410(1983)109:1(15)).
- 354 Bullock RL (2011) Subsurface mine development. In Darling P (ed) Sme Mining Engineering  
355 Handbook, Society for Mining Metallurgy & Exploration. Society for Mining, Metallurgy,  
356 and Exploration, Inc., Englewood, pp 1203-1221.
- 357 Carter PG (2011) Selection Process for Hard-Rock Mining. In Darling P (ed) Sme Mining  
358 Engineering Handbook, Society for Mining Metallurgy & Exploration. Society for Mining,  
359 Metallurgy, and Exploration, Inc., Englewood, pp 357-376.
- 360 Fenner R (1939) Untersuchungen zur Erkenntnis des Gebirgsdruckes. Glueckauf 74: 32-33.

361 Guo Z, Yang X, Bai Y, Zhou F, Li E (2012) A study of support strategies in deep soft rock:  
362 The horsehead crossing roadway in Daqiang Coal Mine. *Int J Min Sci Tech* 22: 665–  
363 667. doi: [10.1016/j.ijmst.2012.08.012](https://doi.org/10.1016/j.ijmst.2012.08.012).

364 Hoek E, Brown ET (1980) *Underground Excavations in Rock*. Institution of Mining and Metal-  
365 lurgy, London.

366 ITASCA (2008) *Flac 6.0 Fast Lagrangian Analysis of Continua, Version 6.0-User's Manual*.  
367 ITASCA Consulting Group Inc: Minneapolis

368 Jia YD, Stace R, Williams A (2013). Numerical modelling of shaft lining stability at deep mine.  
369 *Min Tech* 122:8-19.

370 McCreath DR (1980) Analysis of formation pressure on tunnel and shaft linings. MEng thesis,  
371 University of Alberta.

372 Öztürk H, Ünal E (2001) Estimation of lining thickness around circular shafts. *Proc 17th In-*  
373 *ternational Mining Congress and Exhibition of Turkey- IMCET2001*, pp 437-444.

374 Oreste P (2005a) A probabilistic design approach for tunnel supports. *Comput. Geotech* 32:  
375 520-534. doi: [10.1016/j.compgeo.2005.09.003](https://doi.org/10.1016/j.compgeo.2005.09.003).

376 Oreste P (2005b) Back-analysis techniques for the improvement of the understanding of rock  
377 in underground constructions. *Tunn Undergr Sp Tech* 20: 7-21. doi:  
378 [10.1016/j.tust.2004.04.002](https://doi.org/10.1016/j.tust.2004.04.002).

379 Oreste P (2009a) The convergence-confinement method: Roles and limits in modern geo-  
380 mechanical tunnel design. *Am J Applied Sci* 6: 757-771. doi:  
381 [10.3844/ajassp.2009.757.771](https://doi.org/10.3844/ajassp.2009.757.771).

382 Oreste P (2009b) The determination of the tunnel structure loads through the analysis of the  
383 interaction between the void and the support using the convergence-confinement  
384 method. *Am J Applied Sci* 11: 1945-1954. doi: [10.3844/ajassp.2014.1945.1954](https://doi.org/10.3844/ajassp.2014.1945.1954)

385 Pacher F (1964) Measurements of deformations in a test gallery as a means of investigating  
386 the behaviour of the rock mass and specifying lining requirements. *Felsmechanik und*  
387 *Ingenieurgeologie, Supplement I*:149- 161.

388 Panet M (1995) Le calcul des tunnels par la méthode convergence-confinement. Presses de  
389 l'école nationale des Ponts et chaussées, Paris.

390 Prater G (1977) An examination of some theories of earth pressure on shaft linings. Can  
391 Geotech J 14:91-106. doi: [10.1139/t77-007](https://doi.org/10.1139/t77-007).

392 Rechsteiner GF, Lombardi G (1974) Une méthode de calcul elasto-plastique de l'état de ten-  
393 sion et de déformation autour d'une cavité souterraine. Proc 3rd Congress of the Inter-  
394 national Society for Rock Mechanics, (ISRM 74), pp 1049-1054.

395 Rostami J (2011) Mechanical rock breaking. In Darling P (ed) Sme Mining Engineering Hand-  
396 book, Society for Mining Metallurgy & Exploration. Society for Mining, Metallurgy, and  
397 Exploration, Inc., Englewood, pp 417-434.

398 Terzaghi K (1943) Theoretical soil mechanics. John Wiley and Sons, New York.

399 Vlachopoulos N, Diederichs MS (2009) Improved longitudinal displacement profiles for con-  
400 vergence confinement analysis of deep tunnels. Rock Mech Rock Eng 42: 131-146.  
401 doi: [10.1007/s00603-009-0176-4](https://doi.org/10.1007/s00603-009-0176-4).

402 Wong RCK, Kaiser PK (1988) Design and performance evaluation of vertical shafts: rational  
403 shaft design method and verification of design method. Can Geotech J 25:320-337.  
404 doi: [10.1139/t88-034](https://doi.org/10.1139/t88-034).

405

406 **Figure caption**

407 Fig. 1 Convergence-confinement curve of an underground opening and the reaction line of  
408 the support (modified after [19]). Key:  $p_0$  is the lithostatic stress,  $u_{R0}$  is the radial wall dis-  
409 placement in the point along the cavity axis where the lining is constructed,  $u_{Rmax}$  is the final  
410 radial wall displacement of the cavity,  $\sigma_{Req}$  is the final radial load on the lining.

411 Fig. 2. Two-dimensional numerical model of the plane section. Left: the whole model; Right:  
412 a detail of the zone close to the shaft wall.

413 Fig 3. Relationship between the radial displacement of the shaft wall  $u_R$  and the internal  
414 pressure for the studied case  $\sigma_R$  obtained by the numerical modeling of the cross-section

415 Fig 4. Element mesh of the axisymmetric numerical model of the half shaft longitudinal sec-  
416 tion: the global view and a detail of the zone of the model close to the temporary shaft bot-  
417 tom.

418 Fig 5 Deformation condition of the shaft in the radial direction, with the presence of lining, in  
419 the section already excavated with different step values,  $s$ . Key:  $u_R$  is the radial displacement  
420 of the shaft wall,  $u_{Rmax}$  is the maximum radial displacement at a great distance from the shaft  
421 bottom,  $R$  is the shaft radius.

422 Fig 6. Plastic zones around the shaft and below the shaft bottom during the axisymmetric  
423 numerical calculation: a final plastic radius  $R_{pl}$  in the interval between 3.75 m and 4.05 m can  
424 be estimated by the results.

425 Fig. 7. Comparison of the trends of radial displacements of shaft wall with the distance  $x$  from  
426 the temporary shaft bottom, obtained by the numerical simulation and Vlachoupulos and  
427 Diederichs formulation. Key: LDP: longitudinal displacement profile; LDP  $R_{pl}$  3.75: displace-  
428 ment profile obtained by the Vlachoupulos and Diederichs formulation considering a plastic  
429 radius of 3.75 m; LDP  $R_{pl}$  4.05: displacement profile obtained by the Vlachoupulos and  
430 Diederichs formulation considering a plastic radius of 4.05 m; LDP  $s=0.6$ : displacement pro-  
431 file obtained by the step by step axisymmetric numerical calculation for a step length of 0.6m;



432 LDP simplified: displacement profile obtained by the simplified axisymmetric numerical calcu-  
433 lation.

434 Fig. 8. Comparison of the applied internal pressure-radial displacement of the wall shaft  
435 curve, obtained with FLAC numerical modelling (dotted line) and with the CCM (continuous  
436 line).

437 Fig. 9. Comparison of the support reaction lines obtained with different calculation proce-  
438 dures. Key: CC: convergence-confinement curve obtained by CCM; CCM: support reaction  
439 line located on the basis of the iterative procedure of section 3; "Flac s=0.3 m": support reac-  
440 tion line located on the basis of step by step procedure using the axisymmetric numerical  
441 model and a step length of 0.3 m; "Flac s=0.6 m": step length of 0.6 m; "Flac s=1.2 m": step  
442 length of 1.2 m; "Flac simplified": support reaction line located on the basis of the simplified  
443 procedure using the axisymmetric numerical model.

444 Fig. 10. Calculation of the final plastic radius  $R_{pl}$  obtained with different calculation proce-  
445 dures. Key: "CCM": plastic radius vs internal pressure curve obtained by CCM; " $\sigma_{Req}$  by-  
446 CCM": plastic radius obtained by the internal pressure derived by the analytical iterative pro-  
447 cedure; " $\sigma_{Req}$  by simplified num. modelling": plastic radius obtained by the internal pressure  
448 derived by the simplified axisymmetric numerical model; " $\sigma_{Req}$  by simplified num. modelling  
449 (s=0.6)": plastic radius obtained by the internal pressure derived by the step by step axisim-  
450 metric numerical model; "Min. value by num. modelling": the plastic radius value obtained by  
451 the axisymmetric numerical analyses.